Published in final edited form as:
Int J Cancer. 2009 March 1; 124(5): 1045–1053. doi:10.1002/ijc.24028.

Functional Significance of VEGFR-2 on Ovarian Cancer Cells

Whitney A. Spannuth[1], **Alpa M. Nick**, **Nicholas B. Jennings**[1], **Guillermo N. Armaiz-Pena**[1], **Lingegowda S. Mangala**[1], **Christopher G. Danes**[1], **Yvonne G. Lin**[1], **William M. Merritt**[1], **Premal H. Thaker**[4], **Aparna A. Kamat**[1], **Liz Y. Han**[1], **James R. Tonra**[5], **Robert L. Coleman**[1], **Lee M. Ellis**[2,3], and **Anil K. Sood**[1,2]

[1] Department of Gynecologic Oncology, The University of Texas M.D. Anderson Cancer Center, Houston, TX

[2] Department of Cancer Biology, The University of Texas M.D. Anderson Cancer Center, Houston, TX

[3] Department of Surgical Oncology, The University of Texas M.D. Anderson Cancer Center, Houston, TX

[4] Department of Gynecologic Oncology, Washington University, St. Louis, MO

[5] ImClone Systems Inc., New York, NY

Abstract

Vascular endothelial growth factor receptor (VEGFR) has recently been discovered on ovarian cancer cells, but its functional significance is unknown and is the focus of the current study. By protein analysis, A2780-par and HeyA8 ovarian cancer cell lines expressed VEGFR-1 and HeyA8 and SKOV3ip1 expressed VEGFR-2. By *in situ* hybridization (ISH), 85% of human ovarian cancer specimens showed moderate to high VEGFR-2 expression while only 15% showed moderate to high VEGFR-1 expression. By immunofluorescence, little or no VEGFR-2 was detected in normal ovarian surface epithelial cells, whereas expression was detected in 75% of invasive ovarian cancer specimens. To differentiate between the effects of tumor *versus* host expression of VEGFR, nude mice were injected with SKOV3ip1 cells and treated with either human VEGFR-2 specific antibody (1121B), murine VEGFR-2 specific antibody (DC101), or the combination. Treatment with 1121B reduced SKOV3ip1 cell migration by 68% ($p < 0.01$) and invasion by 72% ($p < 0.01$), but exposure to VEGFR-1 antibody had no effect. Treatment with 1121B effectively blocked VEGF-induced phosphorylation of p130Cas. *In vivo*, treatment with either DC101 or 1121B significantly reduced tumor growth alone and in combination in the SKOV3ip1 and A2774 models. Decreased tumor burden after treatment with DC101 or 1121B correlated with increased tumor cell apoptosis, decreased proliferative index, and decreased microvessel density. These effects were significantly greater in the combination group ($p<0.001$). We show functionally active VEGFR-2 is present on most ovarian cancer cells. The observed anti-tumor activity of VEGF-targeted therapies may be mediated by both anti-angiogenic and direct anti-tumor effects.

Keywords

VEGFR; angiogenesis; ovarian carcinoma

Address correspondence and reprint requests to: Anil K. Sood, M.D., Professor, Departments of Gynecologic Oncology and Cancer Biology, Unit 1362, P.O. Box 301439, Houston, TX 77230-1439. Phone: (713) 745-5266; Fax: (713) 792-7586; Email: asood@mdanderson.org.

INTRODUCTION

Ovarian cancer is the second most common gynecologic cancer in women and remains the most common cause of death from gynecologic malignancy, with over 15,000 deaths per year 1. Approximately 75% of women are diagnosed with advanced stage disease due to lack of early warning signs and effective screening tools 2. Despite high initial response rates to aggressive primary therapy, most ovarian cancers develop drug resistance resulting in eventual patient demise3. Unfortunately, the 5-year survival rate for these patients has not risen above 20–25% 4. There is hence a critical need to develop better therapeutic agents and strategies.

Angiogenesis is a complex, highly regulated process that is critical for tumor growth and metastasis. This dynamic process is regulated by a number of pro- and anti-angiogenic molecules. VEGF-A (commonly noted as VEGF) is one of many proangiogenic factors and has been identified as the predominant growth factor expressed by tumor cells 5. VEGF expression is regulated by several factors including hypoxia, acidosis, mechanical stress, and alterations in oncogenes and tumor suppressor genes, and is known to promote endothelial proliferation, migration, survival, differentiation, and vascular permeability 6.

Overexpression of VEGF occurs in most solid tumors including breast, lung, colon, uterus, and ovarian cancers, and has been associated with tumor progression and poor prognosis 7–10. Several studies have shown a significant increase in serum VEGF levels in patients with ovarian cancer compared to healthy individuals 7, 11, 12. VEGF overexpression has been associated with a shortened disease-free survival 7 and overall survival in ovarian cancer 11. In addition, elevated preoperative serum VEGF levels have been shown to be an independent prognostic factor in patients with ovarian cancer 13. While VEGF-targeted therapies show promise in the clinical setting, their mechanism of action is not fully understood. The VEGF ligand has specific binding affinities to VEGF receptor (VEGFR) -1 and VEGFR-2. VEGFR-2 on the endothelial cells is thought to be the major mediator of angiogenesis in solid tumors and has been a receptor of focus for a number of anti-angiogenic agents currently in clinical investigation. Of particular interest, is the recent discovery of VEGFRs on tumor cells, suggesting an autocrine VEGF/VEGFR pathway 14–16. A functional VEGF/VEGFR autocrine loop has been identified in subsets of human leukemias as well as cancers of the breast, prostate, colon, and skin (melanoma) 17–21. In a lymphoma xenograft model, targeting tumor-associated VEGFR-1 (human lymphoma cells) increased apoptosis, while targeting host (murine) VEGFR-2 decreased microvascular density 22. In a breast cancer model, VEGFR-1 inhibition on tumor cells was effective in blocking tumor growth. Importantly, combination treatment with monoclonal antibodies (mAbs) targeting human VEGFR-1 on tumor cells and murine VEGFR-1 on vasculature had an additive effect in decreasing tumor growth and angiogenesis17. While VEGFR-2 expression on ovarian cancer cells has been reported 23–25, its functional significance is not known.

The purpose of this study was to evaluate the functional role of VEGFRs on ovarian cancer cells. To differentiate between VEGF-mediated autocrine and paracrine effects *in vivo*, nude mice engrafted with human ovarian cancer cells were treated with species-specific antibodies against human VEGFR-2 (1121B) or murine VEGFR-2 (DC101). Signaling mechanisms responsible for anti-tumor effects were also evaluated.

MATERIALS AND METHODS

Cell culture

The ovarian cancer cell lines SKOV3ip1, A2780-par, A2774, and HeyA8 26 were maintained and propagated *in vitro* by serial passage in RPMI-1640 supplemented with 15% fetal bovine serum and 0.1% gentamicin sulfate (Gemini Bioproducts, Calabasas, CA). All of the cell lines were routinely screened for *Mycoplasma* species (GenProbe detection kit; Fisher, Itasca, IL). All of the experiments were performed at 70–80% confluence.

Reagents

Primary antibodies were purchased from the following manufacturers: rabbit anti-VEGFR-2 (Flk-1; Santa Cruz Biotechnology, Santa Cruz, CA); rabbit anti-VEGFR-2 Tyr (Santa Cruz Biotechnology); phospho-p42/44 Erk (Cell Signaling Technology, Danvers, MA); phospho-PI3K (Cell Signaling Technology), phospho-p130Cas (Cell Signaling Technology); phospho-STAT3 (Cell Signaling Technology); phospho-paxillin (Epitomics, Burlingame, CA). Human recombinant human growth factors were purchased from the following manufacturers: VEGF-A (Invitrogen, Carlsbad, CA) and VEGF-B (R&D Systems, Minneapolis, MN). Human monoclonal VEGFR-1 (18F1) and VEGFR-2 (1121B) antibodies as well as the murine monoclonal VEGFR-2 (DC101) antibody were kindly gifted from ImClone Systems (New York, NY) and were used for *in vitro* and *in vivo* inhibition.

Western blot

For evaluation of VEGFR-1 and VEGFR-2 expression, cell lysate was prepared from ovarian cancer cells in log growth phase at 70% confluency. VEGFR-2 phosphorylation was assessed following serum starvation of cells for 24 hrs and subsequent serum replacement for various time periods (0 min, 15 min, 30 min, and 4 hrs). For evaluation of VEGFR-2 inhibition, cells were serum starved overnight and then exposed to VEGFR-2 blocking antibody 1121B (20 μg/ml) for 2 hrs at 37°C. VEGF-A (10 ng/ml) or PBS control was added and cell lysates were collected at various time points. All cultured cell lysates were prepared by washing in PBS and then incubating in modified radioimmunoprecipitation assay (RIPA) lysis buffer with 1 X protease inhibitor (Roche, Mannheim, Germany) and 1mM sodium orthovanadate for 20 minutes on ice. Cells were removed from plates by scraping and then collected for centrifuge at 13,000 rpm for 20 minutes at 4°C. The protein concentration of the samples was determined by a bicinchoninic acid Protein Assay Reagent kit. Typically, 50 μg of protein from whole-cell lysate were fractionated by 10% SDS-PAGE, transferred to nitrocellulose, blocked with 5% nonfat milk for 1h at room temperature, and probed with primary antibody at 4°C overnight. Blots were then incubated with horseradish peroxidase-conjugated anti-mouse or anti-rabbit secondary antibody (1:2000; The Jackson Laboratory, Bar Harbor, ME). Blots were developed with use of an enhanced chemiluminescence detection kit (ECL; Amersham Pharmacia Biotech, Piscataway, NJ). To ensure equal protein loading, a monoclonal actin antibody (1:2000; Chemicon International, Temecula, CA) was used.

Patient samples

After approval by the M.D. Anderson Cancer Center Institutional Review Board for the Protection of Human Subjects, 28 formalin-fixed, paraffin-embedded human ovarian cancer samples and 6 normal ovarian surface epithelium samples were collected. All of the patients underwent surgical exploration and cytoreduction as the initial treatment. The treating gynecologic oncologist determined the adjuvant therapy. Diagnosis was verified by a pathology review at the institutional gynecologic oncology tumor board. All of the patients were staged according to the International Federation of Gynecology and Obstetrics surgical

staging system. A gynecologic pathologist reviewed all of the pathology results for all of the patients.

RT-PCR

Total RNA was isolated and prepared from HeyA8, A2780-par, and SKOV3ip1 cells using the RNAeasy minikit (Qiagen, Valencia, CA) according to the manufacturer's instructions. cDNA was synthesized from 5 μg of total RNA using the Superscript First-Strand Kit (Invitrogen) as per manufacturer's instructions. cDNA was subjected to reverse transcription polymerase chain reaction (RT PCR) for VEGFR-1 and VEGFR-2 with β-Actin as a housekeeping gene. The sequence of primers used are as follows: VEGFR-1 sense: 5′-CGACGAATTGACCAAAGCAA-3′, antisense: 5′-CGGCCTTTTCGTAAATCTGG-3′; VEGFR-2 sense: 5′-GCTCAAGACAGGAAGACCAA-3′, antisense: 5′-ACTTTTGCACAGCCAAGAAC-3′. The PCR cycling conditions for VEGFR-1 were as follows: 94 °C for 2 minutes, followed by 35 cycles of 94 °C for 30 seconds, 60 °C for 45 seconds, and 72 °C for 2 minutes. The PCR cycling conditions for VEGFR-2 were as follows: 94 °C for 5 minutes, followed by 35 cycles of 94 °C for 45 seconds, 54 °C for 1 minute, and 70 °C for 45 seconds. Amplified PCR products were analyzed by electrophoresis on 1% agarose gel with Tris-borate-EDTA buffer and visualized under UV light after staining with ethidium bromide.

Immunohistochemistry staining of proliferating cell nuclear antigen (PCNA), CD31, and TUNEL

For immunohistochemical analysis, paraffin-embedded tissues were sectioned (5-μm-thick) and used to detect expression of proliferating cell nuclear antigen (PCNA), and terminal deoxyribonucleotide transferase mediated nick-end labeling (TUNEL). Frozen sections were used for detecting CD31. Generally, formalin-fixed, paraffin-embedded sections were deparaffinized by sequential washing with xylene, 100% ethanol, 95%ethanol, 80% ethanol, and PBS. After antigen retrieval, endogenous peroxidases were blocked with 3% H_2O_2 in methanol for 5 min. After PBS washes, slides were blocked with 5% normal horse serum and 1% normal goat serum in PBS for 15 minutes at room temperature, followed by incubation with primary antibody in blocking solution overnight at 4°C. Next, the appropriate secondary antibody conjugated to horseradish peroxidase (HRP) in blocking solution was added for 1 hour at room temperature. HRP was detected with 3,3′-diaminobenzidine (DAB; Phoenix Biotechnologies, Huntsville, AL) substrate for 5 minutes, washed, and counterstained with Gill's no. 3 hematoxylin (Sigma). Primary antibodies used included anti-CD31 (platelet/endothelial cell adhesion molecule 1, rat IgG; PharMingen, San Diego, CA), anti-VEGF (rabbit IgG; Santa Cruz Biotechnology Inc., Santa Cruz, CA), and anti-PCNA (PC-10, mouse IgG; DAKO, Carpinteria, CA) using the appropriate secondary HRP-conjugated antibody; followed by development with DAB. Antigen retrieval for studies on paraffin-embedded slides was done by microwave heating for 5 minutes in 0.1 mol/L citrate buffer (pH 6.0; for PCNA). After endogenous peroxidase block, slides were incubated with 0.13 μg/mL mouse IgG Fc blocker (The Jackson Laboratory, Bar Harbor, ME) for 2 hours before primary antibody incubation. Immunohistochemistry for CD31 was performed on freshly cut frozen tissue. These slides were fixed in cold acetone for 10 minutes and did not require antigen retrieval. For TUNEL staining, after deparaffinizing, samples were treated with proteinase K (1:500 dilution) and rinsed with distilled water. One set of slides was treated with DNase (1:50 dilution) as a positive control. Samples were incubated with terminal (1:400) and biotin-16-dUTP (1:200) in terminal deoxynucleotidyl transferase buffer at 37°C for 1 hour and then incubated with 2% bovine serum albumin/ normal horse serum in double-distilled water. Samples were incubated with peroxidase streptavidin 1:400 in house detection diluent at 37°C for 40 minutes. A positive reaction was indicated by a reddish-brown precipitate in the nucleus. Images were captured with the use

of a three chip camera (Sony Corporation of America, Montvale, NJ) and Optimas Image Analysis software (Bioscan, Edmond, WA). Staining for PCNA, CD31, and TUNEL was conducted on tumors collected at the conclusion of 4-week therapy trials. For quantification of PCNA or TUNEL expression, the number of PCNA- or TUNEL-positive tumor cells were counted in 10 random fields at X200 magnification. To quantify microvessel density, microvessel-like structures consisting of endothelial cells that were stained with the anti-CD31 antibody were counted in similar fields.

Immunoflourescence

Fresh frozen ovarian tumors were cut into 8 μm sections and mounted on positively charged slides. Sections were fixed in cold acetone for 10 minutes and then washed with PBS. Slides were blocked with 4% cold water fish skin gelatin in PBS. Samples were then incubated overnight with VEGFR-2 or p-VEGFR-2 primary antibody (Calbiochem, Darmstadt, Germany) at 4°C (1:400, 1:600 dilution). Slides were then incubated with the corresponding fluorescent secondary antibody goat anti-rabbit Alexa 488 for 1 hour at room temperature (1:600 dilution). After PBS washes, Hoechst nuclear counterstain was applied.

In situ hybridization

VEGFR mRNA levels were assessed in formalin-fixed, paraffin-embedded tissue from the short-term experiment on established tumors described above that had been sectioned and mounted on ProbeOn slides using the Microprobe manual system (Fisher Scientific, Pittsburgh, PA). Slides were deparaffinized and rehydrated as described above and subjected to enzymatic digestion with pepsin (Dako) for 20 minutes at 37°C. Slides were incubated with a biotinylated VEGFR probe (1:200 dilution in PBS) for 60 minutes at 45°C. They were then washed three times, for 2 minutes each, in 2× SSC at 45°C, incubated with alkaline phosphatase labeled avidin (Dako) for 30 minutes at 45°C, rinsed in 50 mM Tris HCl buffer (pH 7.6), exposed to alkaline phosphatase enhancer (Biomeda Corp, Foster City, CA) for 1 minute, and finally incubated with Fast Red chromagen substrate (Research Genetics, Carlsbad, CA) for 30 minutes at 45°C. Red staining indicates a positive reaction. Concurrent controls were performed. The negative control included all steps, with elimination of biotinylated probe from the hybridization reaction. The positive control used a poly(dT) 20 oligonucleotide, which provided both confirmation of mRNA integrity and a comparison group for analysis of stain intensity. All samples, including controls, were tested together in a single experimental run. For imaging analysis, regions at the periphery of the tumor, representing the areas of greatest staining, were compared between groups. Four photographs of each slide were taken. Ten areas of each photograph were selected at random, and the histogram output of mean staining intensity using the histogram tool in Adobe Photoshop was recorded as intensity of staining. Both the intensity of staining as given by histogram measurement and a “relative” score are given. For relative scoring, the absolute intensity measurement for the negative control is designated zero and the absolute intensity measurement for the positive control is designated 100, with relative intensity scores for experimental samples calculated based on these reference points.

Migration assay

To determine the effects of human VEGFR-1 and VEGFR-2 blockade on tumor cell migration, 1×10^5 tumor cells, pretreated with VEGFR-1 or VEGFR-2 mAb for 24 hrs, were resuspended in serum-free media (SFM) and plated onto a 0.1% gelatin coated membrane matrix using a membrane culture system 13. Bottom wells were filled with SFM or SFM + VEGF-A (10 ng/ml) as a chemoattractant. Chambers were incubated for 6 hours at 37°C. At completion, cells in bottom chambers were removed with 0.1% EDTA, loaded onto a 3.0 micron polycarbonate filter (Osmonics, Livermore, CA) using an S&S Minifold I Dot-Blot System (Schleicher & Schuell, Keene, NH), fixed, stained, and counted by light

microscopy 13. Cells from ten random fields (final magnification= 400×) were counted by two investigators (W.A.S. and A.K.S) and quantified as a percentage of migrated cells/1 × 10^5 cells plated. Experiments were performed in duplicate.

Invasion Assay

The effect of VEGFR-1 and VEGFR-2 blockade on tumor cell invasion was performed using a membrane invasion culture system as previously described 13. In brief, SKOV3ip1, A2780-par, or HeyA8 cells were pretreated with antibody for 24 hours. The following day, 1 × 10^5 viable cells (resuspended in SFM) were placed into the top wells onto a membrane uniformly coated with a matrix consisting of human laminin (Sigma), type IV collagen (Sigma), and gelatin (ICN Biomedical, Aurora, CO). SFM was placed into bottom wells as chemoattractant and chambers were then incubated for 24 hours at 37°C. Analysis of invaded cells was performed as previously described for migration assay. The invasion assays were performed in duplicate and repeated once.

Cell proliferation assay

In order to determine the *in vitro* effects of VEGFR-2 blockade on the growth of ovarian cancer cells, 2,000 cells per well were plated in a 96-well plate with experimental conditions set in triplicate. Cells were then subjected to sequentially diluted concentrations of 1121B, with and without VEGF-A stimulation (10 ng/ml) and then incubated for 72 hours at 37°C. To assess for cell viability, 50 μL of 0.15% 3-(4,5-dimethylthiazol-2-yl)-2,5-diphenyltetrazolium bromide (Sigma) was added to each well, and incubated for 2 hours at 37°C. The medium/3-(4,5-dimethylthiazol-2-yl)-2,5-diphenyltetrazolium bromide preparation was then removed from each well, and 100 μL of DMSO (Sigma) was added. Absorbance was read at 570 nm absorbance (Ceres UV 900C, Bio-Tek Instrument, Inc., Winooski, VT) within 30 minutes.

Orthotopic ovarian cancer mouse model

Female athymic nude mice (NCr-nu) were purchased from the Animal Production Area of the National Cancer Institute-Frederick Cancer Research and Development Center. The mice were housed and maintained under specific pathogen-free conditions in facilities approved by the American Association for Accreditation of Animal Care in accordance with current regulations and standards of the United States Department of Agriculture, United States Department of Health and Human Services, and the National Institutes of Health. The mice were used according to institutional guidelines when they were 8–12 weeks of age. SKOV3ip1, A2774, and A2780-par tumor cells were harvested from sub-confluent cultures by a brief exposure to 0.25% trypsin. Trypsin was neutralized with FBS-containing medium. The cells were then washed once in serum-free medium and reconstituted in serum-free Hank's balanced salt solution (Life Technologies, Carlsbad, CA) at a concentration of 5 × 10^6 cells/ml for 200 μL i.p. injections. Only single-cell suspensions with greater than 95% viability, as determined by trypan blue exclusion, were used for the injections. Seven days after tumor cell injection, mice were randomized into four groups (n = 10/group), and the following treatments were initiated as 200 μL, intraperitoneal (IP) injections: control IgG (1 mg twice weekly), 1121B (1 mg twice weekly), DC101 (800 μg once weekly), or 1121B and DC101 in combination (1 mg twice weekly and 800 μg once weekly) for 4 weeks. Mice were sacrificed 28 to 42 days after tumor cell injection, at which time body weight was recorded. Tumors in the peritoneal cavity were excised and weighed. For immunohistochemical staining and H&E staining procedures, tumors were fixed in formalin and embedded in paraffin. For immunofluorescence staining, terminal deoxynucleotidyl transferase mediated dUTP nick-end labeling (TUNEL) and immunohistochemistry requiring frozen tissue, tumors were embedded in OCT compound (Miles, Inc.), frozen rapidly in liquid nitrogen, and stored at −80°C.

Statistical analysis

All measurements are depicted as the average ± SE of the mean. Continuous variables were compared with the Student's t test or ANOVA if normally distributed and the Mann-Whitney rank sum test if distributions were nonparametric using Statistical Package for the Social Sciences (SPSS, Inc.). A p-value of < 0.05 was considered statistically significant.

RESULTS

VEGFR expression in ovarian carcinoma

Prior to performing functional assays, we first characterized VEGFR expression in the ovarian cancer cells. RT-PCR revealed that VEGFR-1 was present in the HeyA8, SKOV3ip1, and A2780-par ovarian cancer cells (Fig. 1*a*). VEGFR-2 was detected only in the HeyA8 and SKOV3ip1 cell lines (Fig. 1*a*). With regard to protein expression, variable VEGFR-1 expression was noted in A2780-par and SKOV3ip1 cell lines, and VEGFR-2 was detected in SKOV3ip1 and HeyA8 cell lines (Fig. 1*b*). VEGFR-2 was also detected in the A2774 ovarian cancer cell line. Murine ovarian endothelial cells (MOECs) were used as a positive control. VEGFR-2 was constitutively phosphorylated in the positive cell lines (data not shown).

We next asked whether VEGFR was also present on the cancer cells from fresh human tumors. Fifteen invasive epithelial ovarian cancer samples were examined for VEGFR expression by *in situ* hybridization. Intensity of staining was obtained using a histogram measurement and reported as a relative score. Low VEGFR expression was designated as <50% staining intensity and moderate to high VEGFR expression as >50% staining intensity of the positive control. Eighty-five percent of ovarian cancer specimens showed moderate to high VEGFR-2 expression while only 15% showed moderate to high VEGFR-1 expression (Fig. 1*c*). Since the human ovarian cancer samples predominantly expressed VEGFR-2, we next tested 28 invasive epithelial ovarian cancer specimens and 6 normal ovarian specimens for VEGFR-2 expression by immunoflourescence. As expected, VEGFR-2 was present and phosphorylated in the tumor vasculature of all samples (data not shown). While little or no VEGFR-2 was detected in epithelial cells of normal ovarian samples, expression was detected in tumor cells from 75% of invasive cancer samples. Moreover, ovarian cancer-cell associated VEGFR-2 was phosphorylated in 71% of ovarian tumor specimens (Fig. 1*d*). Since VEGFR-2 was the predominant receptor in human ovarian cancer samples, we focused on this receptor for further *in vitro* and *in vivo* characterization.

In vitro effects of VEGFR-2 inhibition on ovarian cancer cells

VEGFR-1 has been implicated in colorectal cancer cell migration and invasion 27; however, the role of VEGFR-2 is not fully known. Therefore, to characterize the functional significance of VEGFR on ovarian cancer cells, we examined the effects of VEGFR inhibition on tumor cell migration, invasion, and proliferation *in vitro*. Tumor cells were pretreated with either VEGFR-1 or VEGFR-2 mAb for 24 hrs prior to the assays. Exposure to VEGFR-2 mAb 1121B resulted in a 68% decrease in SKOV3ip1 cell migration compared to cells treated with control Ab ($p < 0.01$; Fig. 2*a*). As expected, treatment with 1121B mAb did not affect migration of A2780-par cells. To examine the effect of VEGFR-2 blockade on chemokine induced migration of ovarian cancer cells, VEGF-A was used as a chemoattractant in the bottom chamber. A 48% increase in SKOV3ip1 cell migration was observed in response to VEGF-A ($p < 0.001$; Fig. 2*b*). The addition of VEGFR-2 mAb 1121B inhibited this increase in migration, confirming that the effect was VEGFR-2 dependent. Treatment with the VEGFR-2 mAb 1121B also significantly decreased SKOV3ip1 tumor cell invasion compared to control (72% reduction, $p < 0.01$: Fig. 2*c*), but again had no effect on the A2780-par cells. The VEGFR-1 mAb had no effect on *in vitro*

tumor cell migration or invasive potential in any of the cell lines. VEGF-A stimulation or treatment with the 1121B antibody had no effect on tumor cell proliferation (data not shown), suggesting that the observed changes in invasion and migration were independent of proliferation.

Anti-human VEGFR-2 mAb suppresses *in vivo* growth of human xenograft ovarian carcinomas

Based on the *in vitro* functional effects of VEGFR-2 mAb, we next asked whether tumor cell VEGFR-2 has implications for tumor growth *in vivo*. For these studies, a well characterized orthotopic mouse model of ovarian carcinoma was utilized. SKOV3ip1 or A2774 bearing animals were randomly assigned to one of the following 4 groups (n=10 mice per group): 1) control antibody, 2) anti-human VEGFR-2 mAb 1121B, 3) anti-mouse VEGFR-2 mAb DC101, and 4) combination of 1121B and DC101. To simulate advanced disease, therapy was initiated 1 week after tumor cell injection. Treatment was continued until control animals exhibited significant tumor burden and became moribund (approximately 4 weeks), at which time all mice in the experiment were sacrificed together. Compared to controls, treatment with the anti-human VEGFR-2 mAb 1121B significantly decreased tumor growth in SKOV3ip1 (44%; $p < 0.05$) and A2774 (62%; $p < 0.05$) cell lines (Fig. 3*a*, *b*). The anti-mouse VEGFR-2 mAb DC101 also significantly decreased tumor growth in both SKOV3ip1 (69%; $p < 0.005$) and A2774 cell lines (76%; $p < 0.005$). Combination therapy with 1121B and DC101 significantly decreased tumor growth in both models (88%, $p < 0.005$; and 86%, $p < 0.005$). Anti-VEGFR-2 treatment also significantly decreased ascites. Treatment with 1121B and DC101 led to an 84% and 88% decrease in ascites in the SKOV3ip1 cell line, respectively. The greatest effect was seen in the combination group, with a 99% decrease in ascites. Similar effects of anti-VEGFR-2 therapy on reduction of ascites were noted in the A2774 model. To test the specificity of effect, we also examined the impact of these antibodies in the VEGFR-2 negative A2780-par model. As anticipated, anti-human VEGFR-2 mAb 1121B did not affect tumor weight compared to control antibody in this model (mean tumor weight 2.11 g versus 1.95 g, $p = 0.14$; Fig. 3*c*). DC101 treatment resulted in a 78% reduction in tumor growth ($p = 0.008$). The effects of combination therapy were similar to treatment with DC101 alone ($p = 0.06$).

Effects of VEGFR-targeted therapy on angiogenesis, proliferation, and apoptosis

To determine the biological effects of treatment with 1121B and DC101, SKOV3ip1 ovarian tumors harvested from mice following therapy were subjected to immunohistochemistry for cell proliferation (PCNA), apoptosis (TUNEL), and mean vessel density (CD31). Treatment with DC101 resulted in a 45% decrease in MVD ($p < 0.001$). Interestingly, even treatment with 1121B resulted in a modest 38% decrease in MVD compared to controls ($p < 0.001$), but the greatest decrease in MVD was noted in the combination group (58% decrease; $p < 0.001$; Fig. 4). There was a 38% reduction in the mean number of PCNA-positive cells in 1121B-treated mice compared to controls and a 42% reduction in mean PCNA-positive cells in DC101-treated mice. The combination of 1121B and DC101 produced the largest reduction in PCNA-positive cells (51%, $p < 0.001$; Fig. 4).

In 1121B-treated mice injected with SKOV3ip1 tumor cells, the mean number of apoptotic tumor cells by TUNEL was increased by 274% compared to controls ($p < 0.001$). Tumors from mice treated with DC101 showed a 247% increase in the number of apoptotic tumor cells ($p < 0.001$), with the largest number of apoptotic cells seen with the combination of 1121B and DC101 (565% increase, $p < 0.001$; Fig. 4).

VEGFR-2 regulates the p130Cas signaling pathway

To elucidate potential mechanisms responsible for the efficacy of VEGFR-targeted therapy, we examined potential effects on signaling pathways involved. Neither stimulation nor inhibition of VEGFR-2 affected phosphorylation of MAPK, PI3K, STAT3, paxillin, or PLC-gamma1 (Fig. 5*a*). We then focused on p130Cas (Crk-associated substrate, Cas) given its observed modulation with both stimulation and inhibition of the receptor in endothelial cells. Assembly of this complex is known to modulate migration, invasion, and cell survival in carcinoma cells 28–30. We found that anti-human VEGFR-2 mAb 1121B inhibited VEGF-mediated phosphorylation of p130CAS in the SKOV3ip1 ovarian cancer cells (Fig. 5*b*). VEGF-A stimulation led to a time-dependent increase in p130Cas phosphorylation (Fig. 5*c*).

DISCUSSION

The key findings in this study include the presence of functionally active VEGFR-2 on ovarian cancer cells and inhibition of autocrine or paracrine VEGFR-2-mediated pathways with species-specific antibodies inhibiting tumor growth in an ovarian cancer model. Suppression of tumor growth was achieved, at least in part, through increased tumor cell apoptosis, and decreased tumor proliferation and vascularization. *In vitro* inhibition of VEGFR-2 on ovarian cancer cells also significantly reduced tumor cell migration and invasion. These anti-tumor effects may be mediated, in part, through the p130Cas signaling pathway.

VEGF-A (VEGF) is a prominent stimulator of angiogenesis and has been implicated in the proliferation and metastasis of a number of malignancies 31–35. It is secreted by most solid tumors and is expressed in > 70% of ovarian carcinomas 23, 24. Elevated VEGF levels in serum and ascitic fluid of patients with ovarian cancer has been correlated with tumor microvessel density (MVD) and stage of malignancy 25, 36. In addition, VEGF expression has been linked to increased tumor aggressiveness and decreased 5-year survival in patients with this disease 24. VEGF normally exerts its effects through binding VEGFR found on endothelial cells, but there is recent evidence for aberrant VEGFR expression on tumor cells. It is conceivable that VEGF increases tumor growth not only by stimulating angiogenesis, but also by direct stimulation of VEGFR expressed on tumor cells. In fact, VEGF-mediated autocrine loops have been identified in breast, colorectal, prostate, and other solid tumor cell lines 15, 17, 18, 20, 21. In a breast cancer xenograft model, inhibiting human VEGFR-1 significantly decreased tumor growth as a result of direct inhibition of VEGFR-1 activation and subsequent downstream kinase signaling. Inhibiting murine VEGFR-1 using a selective anti-murine VEGFR-1 mAb had an additive effect in decreasing tumor growth and angiogenesis 17. In a lymphoma xenograft model, inhibiting autocrine VEGFR-1 pathways or paracrine VEGFR-2 pathways significantly decreased the growth of established tumors by increasing tumor cell apoptosis and decreasing vascularization and endothelial cell number 22. While VEGFRs have recently been identified on ovarian cancer cells, the functional significance of this finding is still unclear.

We hypothesized that the presence of VEGFRs on ovarian cancer cells would allow cells to respond to VEGF through an autocrine signaling pathway. Indeed, inhibition of human VEGFR-2 using a selective anti-human VEGFR-2 mAb (1121B) significantly reduced tumor growth in an established ovarian cancer xenograft model. Decreased tumor growth was mediated, at least in part, through increased apoptosis, and decreased proliferation and vascularization. In addition, targeting murine VEGFR-2 using a selective anti-murine VEGFR-2 mAb (DC101) led to a significant reduction in tumor growth. Combination therapy with 1121B and DC101 had the greatest effect, supporting both an autocrine and paracrine VEGF/VEGFR-2 loop in ovarian cancer. To confirm the specificity of these results, a VEGFR-2 null model A2780-par was evaluated, which demonstrated no effect of

the anti-human VEGFR-2 1121B antibody on tumor growth. Similar results have been shown by Dias and associates using a human leukemia model. Targeting either autocrine or paracrine VEGF/VEGFR-2 pathways delayed leukemic growth and engraftment *in vivo*. Blocking both pathways was necessary to achieve long-term remission or cure 37.

While there is growing evidence that VEGF can directly promote tumor cell proliferation and survival, the underlying cellular processes are not fully understood. We found that treatment with anti-human VEGFR-2 mAb 1121B significantly decreased tumor cell migration and invasion compared to control. Treatment with 1121B also inhibited VEGF-A induced tumor cell migration and invasion. This effect was not seen in the A2780-par cell line that lacks the VEGFR-2 receptor. Exposure to anti-human VEGFR-1 mAb had no effect on tumor cell migration or invasion. The signaling pathways downstream of VEGFR-2 in tumor cells are also not fully understood. In this study, we show increased levels of phosphorylated p130Cas in response to ovarian cancer cell stimulation with VEGF. This phosphorylation was effectively blocked by VEGFR-2 inhibition with the 1121B mAb. Our results are consistent with findings by Endo et al. who showed that VEGFR-2 blockade could reverse VEGF-stimulated phosphorylation of p130Cas in human aortic endothelial cells (HAECs)38. P130Cas is a docking protein that complexes with Crk (CT10 regulator of kinase) upon phosphorylation, leading to the recruitment of various effectors that couple the scaffold to the actin cytoskeleton of the cell 28. Evidence indicates that Cas/Crk assembles at the plasma membrane and focal adhesions to modulate cell migration, invasion, and survival 28–30. Based on these and other studies linking p130Cas to tumor cell invasion and migration, our data provide new insight into underlying mechanisms that link VEGFR-2 on ovarian cancer cells to such aggressive features 39.

Several studies have shown increased VEGFR-2 expression in human ovarian cancer specimens. Inan and coworkers demonstrated increased immunoreactivity of VEGFR-2 in all malignant ovarian tumor samples compared to benign or borderline tumors 40. Nishida and associates demonstrated high tissue expression of VEGFR-2 in 75% of ovarian cancer specimens examined immunohistochemically 24. We found similar results by immunoflourescence, with VEGFR-2 expression detected in a majority of ovarian cancer specimens but largely absent in epithelial cells of normal ovarian samples. However, we extend prior work by demonstrating that VEGFR-2 is phosphorylated on ovarian cancer cells, and VEGFR-2 mRNA is also detected at increased levels in ovarian cancer cells. In contrast to other malignancies such as pancreatic and colorectal cancer 21, 41, 42, VEGFR-1 expression is largely absent in ovarian cancer cells.

In summary, we have demonstrated a functional role for VEGFR-2 in ovarian cancer cells and identified a distinct VEGFR-2-mediated pathway promoting tumor growth through autocrine mechanisms. Targeting VEGFR-2 with anti-human VEGFR-2 mAb 1121B significantly inhibited tumor growth and vascularization *in vivo*, providing further insight into the anti-tumor role of VEGF/VEGFR pathways. In early clinical studies, IMC-1121B (Imclone Systems, New York, NY) is showing promising results where 2 of 12 patients achieved a partial response while seven achieved stable disease 43. Our preclinical results, in addition to phase I study results, support further evaluation of VEGFR-2-targeted therapy in ovarian carcinoma.

Acknowledgments

This work was supported in part by NIH grants (CA110793 and CA199298), and the U.T.M.D. Anderson Ovarian Cancer Spore (P50 CA083639-06) awarded to AKS. WMM, YGL, and WAS are supported by the National Cancer Institute - DHHS - NIH T32 Training Grant (T32 CA101642).

The authors would like to thank Donna Reynolds, Carol Oborn, and Dr. Robert Langley for assistance with immunohistochemistry and for helpful discussions.

Lee M. Ellis, M.D. has received research support from ImClone Systems Inc. He has also served as a consultant to ImClone Systems. James R. Tonra, Ph.D. is employed by and holds stock in ImClone Systems Inc

References

1. Jemal A, Siegel R, Ward E, Murray T, Xu J, Thun MJ. Cancer statistics, 2007. CA Cancer J Clin. 2007; 57:43–66. [PubMed: 17237035]
2. Partridge EE, Barnes MN. Epithelial ovarian cancer: prevention, diagnosis, and treatment. CA Cancer J Clin. 1999; 49:297–320. [PubMed: 11198956]
3. Agarwal R, Kaye SB. Ovarian cancer: strategies for overcoming resistance to chemotherapy. Nat Rev Cancer. 2003; 3:502–16. [PubMed: 12835670]
4. Ozols RF. Treatment goals in ovarian cancer. Int J Gynecol Cancer. 2005; 15 (Suppl 1):3–11. [PubMed: 15839952]
5. Dvorak HF. Vascular permeability factor/vascular endothelial growth factor: a critical cytokine in tumor angiogenesis and a potential target for diagnosis and therapy. J Clin Oncol. 2002; 20:4368–80. [PubMed: 12409337]
6. Gasparini G, Longo R, Toi M, Ferrara N. Angiogenic inhibitors: a new therapeutic strategy in oncology. Nat Clin Pract Oncol. 2005; 2:562–77. [PubMed: 16270097]
7. Paley PJ, Staskus KA, Gebhard K, Mohanraj D, Twiggs LB, Carson LF, Ramakrishnan S. Vascular endothelial growth factor expression in early stage ovarian carcinoma. Cancer. 1997; 80:98–106. [PubMed: 9210714]
8. Olson TA, Mohanraj D, Carson LF, Ramakrishnan S. Vascular permeability factor gene expression in normal and neoplastic human ovaries. Cancer Res. 1994; 54:276–80. [PubMed: 8261452]
9. Ohta Y, Tomita Y, Oda M, Watanabe S, Murakami S, Watanabe Y. Tumor angiogenesis and recurrence in stage I non-small cell lung cancer. Ann Thorac Surg. 1999; 68:1034–8. [PubMed: 10510003]
10. Ishigami SI, Arii S, Furutani M, Niwano M, Harada T, Mizumoto M, Mori A, Onodera H, Imamura M. Predictive value of vascular endothelial growth factor (VEGF) in metastasis and prognosis of human colorectal cancer. Br J Cancer. 1998; 78:1379–84. [PubMed: 9823983]
11. Yamamoto S, Konishi I, Mandai M, Kuroda H, Komatsu T, Nanbu K, Sakahara H, Mori T. Expression of vascular endothelial growth factor (VEGF) in epithelial ovarian neoplasms: correlation with clinicopathology and patient survival, and analysis of serum VEGF levels. Br J Cancer. 1997; 76:1221–7. [PubMed: 9365173]
12. Kraft A, Weindel K, Ochs A, Marth C, Zmija J, Schumacher P, Unger C, Marme D, Gastl G. Vascular endothelial growth factor in the sera and effusions of patients with malignant and nonmalignant disease. Cancer. 1999; 85:178–87. [PubMed: 9921991]
13. Cooper BC, Ritchie JM, Broghammer CL, Coffin J, Sorosky JI, Buller RE, Hendrix MJ, Sood AK. Preoperative serum vascular endothelial growth factor levels: significance in ovarian cancer. Clin Cancer Res. 2002; 8:3193–7. [PubMed: 12374688]
14. Decaussin M, Sartelet H, Robert C, Moro D, Claraz C, Brambilla C, Brambilla E. Expression of vascular endothelial growth factor (VEGF) and its two receptors (VEGF-R1-Flt1 and VEGF-R2-Flk1/KDR) in non-small cell lung carcinomas (NSCLCs): correlation with angiogenesis and survival. J Pathol. 1999; 188:369–77. [PubMed: 10440746]
15. Ferrer FA, Miller LJ, Lindquist R, Kowalczyk P, Laudone VP, Albertsen PC, Kreutzer DL. Expression of vascular endothelial growth factor receptors in human prostate cancer. Urology. 1999; 54:567–72. [PubMed: 10475375]
16. Masood R, Cai J, Zheng T, Smith DL, Hinton DR, Gill PS. Vascular endothelial growth factor (VEGF) is an autocrine growth factor for VEGF receptor-positive human tumors. Blood. 2001; 98:1904–13. [PubMed: 11535528]
17. Wu Y, Hooper AT, Zhong Z, Witte L, Bohlen P, Rafii S, Hicklin DJ. The vascular endothelial growth factor receptor (VEGFR-1) supports growth and survival of human breast carcinoma. Int J Cancer. 2006; 119:1519–29. [PubMed: 16671089]

18. Lacal PM, Failla CM, Pagani E, Odorisio T, Schietroma C, Falcinelli S, Zambruno G, D'Atri S. Human melanoma cells secrete and respond to placenta growth factor and vascular endothelial growth factor. J Invest Dermatol. 2000; 115:1000–7. [PubMed: 11121133]

19. Bellamy WT, Richter L, Frutiger Y, Grogan TM. Expression of vascular endothelial growth factor and its receptors in hematopoietic malignancies. Cancer Res. 1999; 59:728–33. [PubMed: 9973224]

20. Jackson MW, Roberts JS, Heckford SE, Ricciardelli C, Stahl J, Choong C, Horsfall DJ, Tilley WD. A potential autocrine role for vascular endothelial growth factor in prostate cancer. Cancer Res. 2002; 62:854–9. [PubMed: 11830543]

21. Lesslie DP, Summy JM, Parikh NU, Fan F, Trevino JG, Sawyer TK, Metcalf CA, Shakespeare WC, Hicklin DJ, Ellis LM, Gallick GE. Vascular endothelial growth factor receptor-1 mediates migration of human colorectal carcinoma cells by activation of Src family kinases. Br J Cancer. 2006; 94:1710–7. [PubMed: 16685275]

22. Wang ES, Teruya-Feldstein J, Wu Y, Zhu Z, Hicklin DJ, Moore MA. Targeting autocrine and paracrine VEGF receptor pathways inhibits human lymphoma xenografts in vivo. Blood. 2004; 104:2893–902. [PubMed: 15238424]

23. Chen H, Ye D, Xie X, Chen B, Lu W. VEGF, VEGFRs expressions and activated STATs in ovarian epithelial carcinoma. Gynecol Oncol. 2004; 94:630–5. [PubMed: 15350351]

24. Nishida N, Yano H, Komai K, Nishida T, Kamura T, Kojiro M. Vascular endothelial growth factor C and vascular endothelial growth factor receptor 2 are related closely to the prognosis of patients with ovarian carcinoma. Cancer. 2004; 101:1364–74. [PubMed: 15368324]

25. Abu-Jawdeh GM, Faix JD, Niloff J, Tognazzi K, Manseau E, Dvorak HF, Brown LF. Strong expression of vascular permeability factor (vascular endothelial growth factor) and its receptors in ovarian borderline and malignant neoplasms. Lab Invest. 1996; 74:1105–15. [PubMed: 8667614]

26. Thaker PH, Yazici S, Nilsson MB, Yokoi K, Tsan RZ, He J, Kim SJ, Fidler IJ, Sood AK. Antivascular therapy for orthotopic human ovarian carcinoma through blockade of the vascular endothelial growth factor and epidermal growth factor receptors. Clin Cancer Res. 2005; 11:4923–33. [PubMed: 16000591]

27. Fan F, Wey JS, McCarty MF, Belcheva A, Liu W, Bauer TW, Somcio RJ, Wu Y, Hooper A, Hicklin DJ, Ellis LM. Expression and function of vascular endothelial growth factor receptor-1 on human colorectal cancer cells. Oncogene. 2005; 24:2647–53. [PubMed: 15735759]

28. Chodniewicz D, Klemke RL. Regulation of integrin-mediated cellular responses through assembly of a CAS/Crk scaffold. Biochim Biophys Acta. 2004; 1692:63–76. [PubMed: 15246680]

29. Klemke RL, Leng J, Molander R, Brooks PC, Vuori K, Cheresh DA. CAS/Crk coupling serves as a "molecular switch" for induction of cell migration. J Cell Biol. 1998; 140:961–72. [PubMed: 9472046]

30. Takino T, Nakada M, Miyamori H, Yamashita J, Yamada KM, Sato H. CrkI adapter protein modulates cell migration and invasion in glioblastoma. Cancer Res. 2003; 63:2335–7. [PubMed: 12727859]

31. Takahashi Y, Kitadai Y, Bucana CD, Cleary KR, Ellis LM. Expression of vascular endothelial growth factor and its receptor, KDR, correlates with vascularity, metastasis, and proliferation of human colon cancer. Cancer Res. 1995; 55:3964–8. [PubMed: 7664263]

32. Fujimoto K, Hosotani R, Wada M, Lee JU, Koshiba T, Miyamoto Y, Tsuji S, Nakajima S, Doi R, Imamura M. Expression of two angiogenic factors, vascular endothelial growth factor and platelet-derived endothelial cell growth factor in human pancreatic cancer, and its relationship to angiogenesis. Eur J Cancer. 1998; 34:1439–47. [PubMed: 9849429]

33. Berns EM, Klijn JG, Look MP, Grebenchtchikov N, Vossen R, Peters H, Geurts-Moespot A, Portengen H, van Staveren IL, Meijer-van Gelder ME, Bakker B, Sweep FC, et al. Combined vascular endothelial growth factor and TP53 status predicts poor response to tamoxifen therapy in estrogen receptor-positive advanced breast cancer. Clin Cancer Res. 2003; 9:1253–8. [PubMed: 12684392]

34. George DJ, Halabi S, Shepard TF, Vogelzang NJ, Hayes DF, Small EJ, Kantoff PW. Prognostic significance of plasma vascular endothelial growth factor levels in patients with hormone-

refractory prostate cancer treated on Cancer and Leukemia Group B 9480. Clin Cancer Res. 2001; 7:1932–6. [PubMed: 11448906]

35. Gorski DH, Leal AD, Goydos JS. Differential expression of vascular endothelial growth factor-A isoforms at different stages of melanoma progression. J Am Coll Surg. 2003; 197:408–18. [PubMed: 12946796]
36. Nakanishi Y, Kodama J, Yoshinouchi M, Tokumo K, Kamimura S, Okuda H, Kudo T. The expression of vascular endothelial growth factor and transforming growth factor-beta associates with angiogenesis in epithelial ovarian cancer. Int J Gynecol Pathol. 1997; 16:256–62. [PubMed: 9421092]
37. Dias S, Hattori K, Heissig B, Zhu Z, Wu Y, Witte L, Hicklin DJ, Tateno M, Bohlen P, Moore MA, Rafii S. Inhibition of both paracrine and autocrine VEGF/VEGFR-2 signaling pathways is essential to induce long-term remission of xenotransplanted human leukemias. Proc Natl Acad Sci U S A. 2001; 98:10857–62. [PubMed: 11553814]
38. Endo A, Fukuhara S, Masuda M, Ohmori T, Mochizuki N. Selective inhibition of vascular endothelial growth factor receptor-2 (VEGFR-2) identifies a central role for VEGFR-2 in human aortic endothelial cell responses to VEGF. Journal of receptor and signal transduction research. 2003; 23:239–54. [PubMed: 14626450]
39. Van Slambrouck S, Grijelmo C, De Wever O, Bruyneel E, Emami S, Gespach C, Steelant WF. Activation of the FAK-src molecular scaffolds and p130Cas-JNK signaling cascades by alpha1-integrins during colon cancer cell invasion. Int J Oncol. 2007; 31:1501–8. [PubMed: 17982677]
40. Inan S, Vatansever S, Celik-Ozenci C, Sanci M, Dicle N, Demir R. Immunolocalizations of VEGF, its receptors flt-1, KDR and TGF-beta's in epithelial ovarian tumors. Histol Histopathol. 2006; 21:1055–64. [PubMed: 16835828]
41. Wey JS, Fan F, Gray MJ, Bauer TW, McCarty MF, Somcio R, Liu W, Evans DB, Wu Y, Hicklin DJ, Ellis LM. Vascular endothelial growth factor receptor-1 promotes migration and invasion in pancreatic carcinoma cell lines. Cancer. 2005; 104:427–38. [PubMed: 15952180]
42. Dallas NA, Fan F, Gray MJ, Van Buren G 2nd, Lim SJ, Xia L, Ellis LM. Functional significance of vascular endothelial growth factor receptors on gastrointestinal cancer cells. Cancer Metastasis Rev. 2007; 26:433–41. [PubMed: 17786539]
43. Camidge DR, Eckhardt SG, Diab S, Gore L, Chow L, O'Bryant C, Temmer E, Ervin-Haynes A, Katz T, Fox F, Cohen RB. A phase I dose-escalation study of weekly IMC-1121B, a fully human anti-vascular endothelial growth factor receptor 2 (VEGFR2) IgG1 monoclonal antibody (Mab), in patients (pts) with advanced cancer [abstract #3032]. J Clin Oncol. 2006; 24(18S)

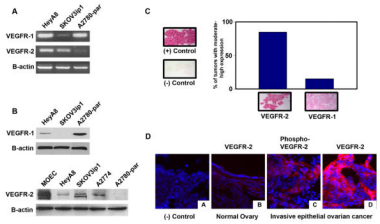

Figure 1.

VEGFR expression on ovarian cancer cell lines and human ovarian tumor samples. (*a*) RT-PCR was performed with mRNA from HeyA8, SKOV3ip1, and A2780-par cell lines. (*b*) Western blot analysis of whole-cell lysates probed with anti-VEGFR-1, anti-VEGFR-2, and anti-actin antibodies. (*c*) *In situ* hybridization for VEGFR. Ovarian cancer specimens were mounted on slides and then incubated with biotinylated probes against VEGFR. Red staining indicates a positive reaction. Concurrent controls were performed. Intensity of staining was obtained using a histogram measurement and reported as a relative score. (*d*) Representative immunoflourescence staining of VEGFR-2 and phospho-VEGFR-2 in ovarian tumor samples.

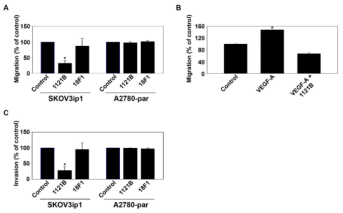

Figure 2.

VEGFR-2 regulates ovarian cancer cell migration and invasion. (a) SKOV3ip1 and A2780-par ovarian cancer cells were pretreated with VEGFR-1 or VEGFR-2 mAb for 24 hours and migration was assessed after 6 hours. (*b*) Invasive potential of SKOV3ip1 and A2780-par cancer cells was assessed following treatment with VEGFR-1 or VEGFR-2 mAb. (*c*) SFM with or without VEGF-A as a chemoattractant was placed in bottom wells and invasion of SKOV3ip1 cells pretreated with 1121B mAb was assessed after 24 hours. *, $p < 0.01$.

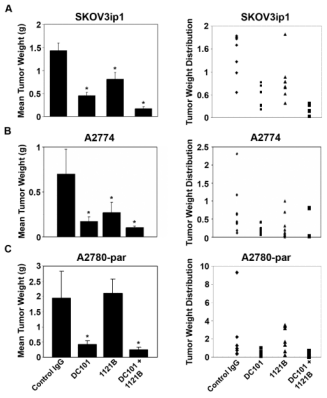

Figure 3.

Therapeutic efficacy of 1121B. Nude mice were injected i.p. with SKOV3ip1, A2774, or A2780-par cells and randomly allocated to one of the following groups (n = 10 per group): IgG control, DC101, 1121B, or DC101 + 1121B. Treatment was started 1 week after tumor cell injection, and mice were sacrificed when control mice became moribund (4–5 weeks following treatment initiation). *, $p<0.05$.

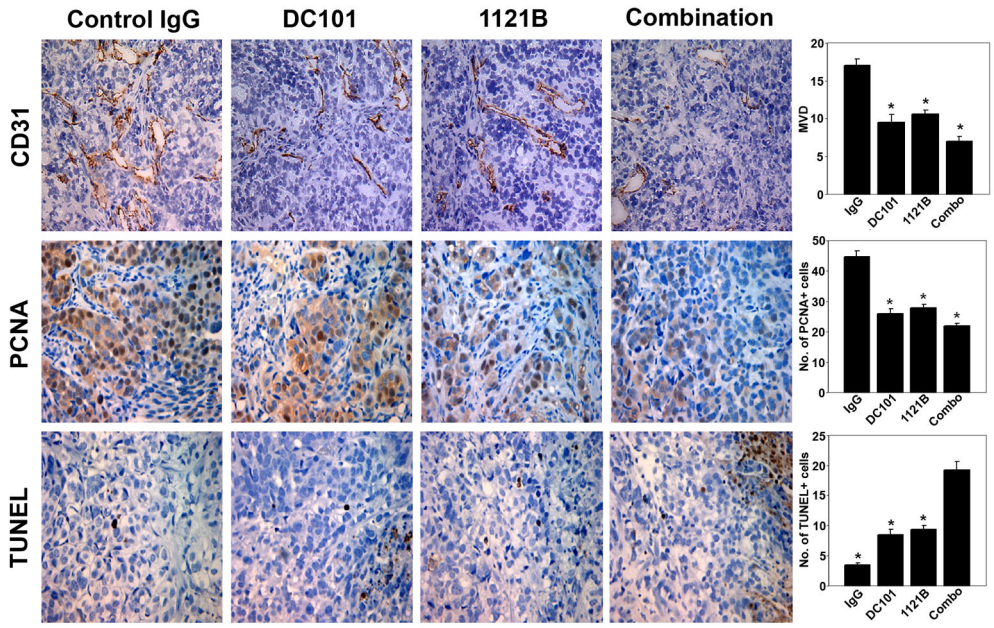

Figure 4.

Proliferation index, microvessel density (MVD), and apoptotic index in tumors treated with DC101, 1121B, or the combination. Representative sections (pictures taken at original magnification, X200) are shown for the various treatment groups. A graphic representation of the average number of CD31-positive vessels per field, mean percentage of PCNA-positive cells, and mean percentage of TUNEL-positive cells are shown in the adjoining graphs. Five slides per group and at least five fields per slide were examined. *, $p<0.001$.

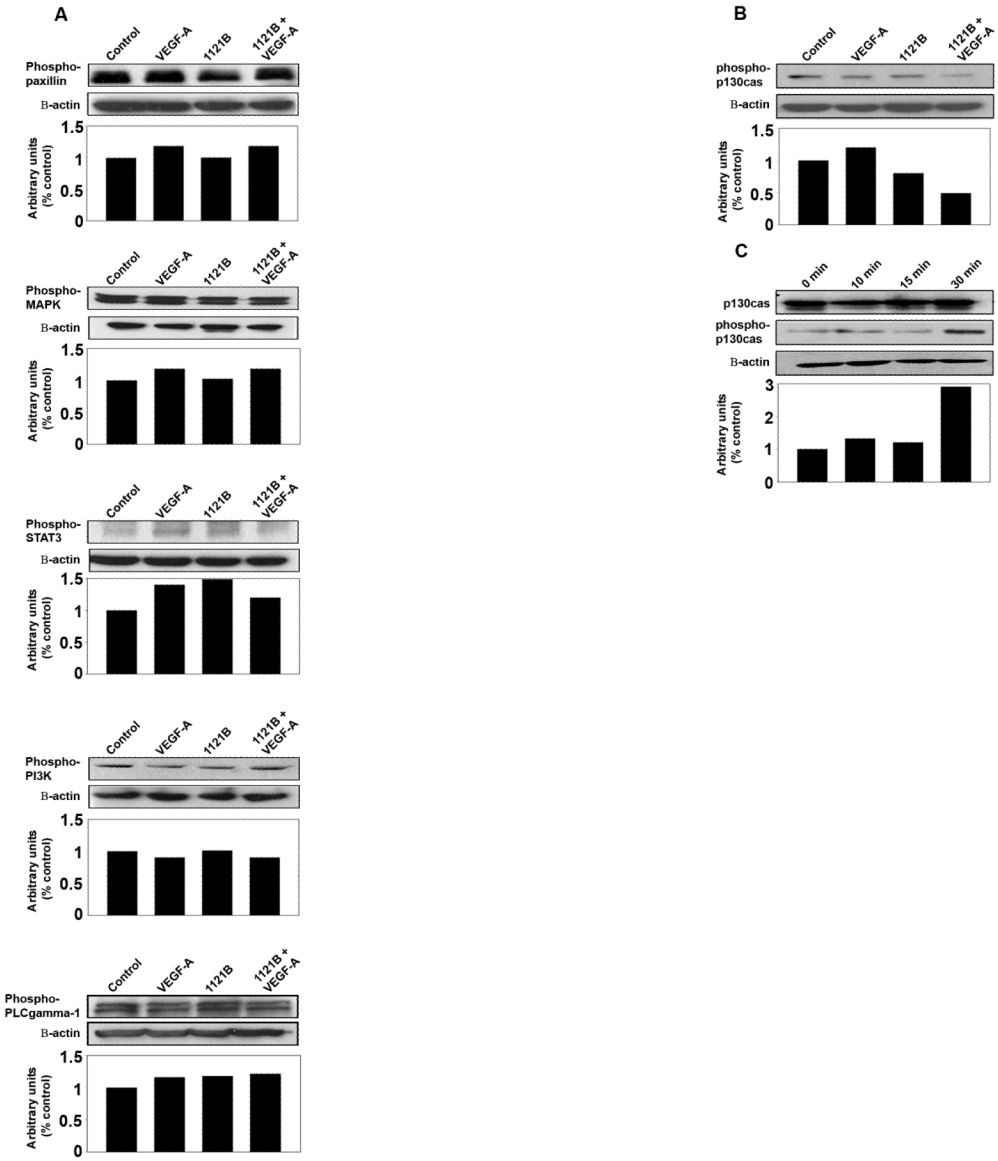

Figure 5.

Effect of VEGFR-2 targeted antibodies on intracellular signaling. SKOV3ip1 ovarian cancer cells were serum starved overnight and then exposed to 1121B (20 μg/ml) for 2 hrs at 37°C. VEGF-A (10 ng/ml) or PBS control was added and cell lysates were collected at various time points. (*a*) Western blot analysis of whole-cell lysates probed with antibody to phosho-paxillin, -MAPK, -PI3K, -STAT3, or PLCgamma1. (*b*) Western blot analysis of lysates probed with antibody to phospho-p130Cas. (*c*) p130Cas phosphorylation following serum starvation of cells for 24 hrs and subsequent VEGF-A (10 ng/ml) stimulation for various time periods (0 min, 15 min, 30 min, and 4 hrs). Whole-cell lysate samples were analyzed for p130Cas and phospho-p130Cas.